Chemical Papers (2023) 77:3603–3617
https://doi.org/10.1007/s11696-023-02723-5

ORIGINAL PAPER

Anticancerous and antioxidant properties of fabricated silver nanoparticles involving bio-organic framework using medicinal plant *Blumea lacera*

Pradeep Kumar Pandey[1] · Chinky Gangwar[1,4] · Bushra Yaseen[1] · Indresh Kumar[1,4] · Rashmi Nayak[2] · Saurabh Kumar[3] · Radhey Mohan Naik[1] · Monisha Banerjee[3] · Joy Sarkar[1]

Received: 26 August 2022 / Accepted: 8 February 2023 / Published online: 21 February 2023
© Institute of Chemistry, Slovak Academy of Sciences 2023

Abstract

Cancer is the second foremost cause of death worldwide, and despite modern medicine development, it is needed to develop new plant-based drugs. The current study is mainly focused on the estimation of anticancerous activity of silver nanoparticles (AgNPs) fabricated by a simple and eco-friendly green approach by using leaf extract of the medicinal plant *Blumea lacera (B. lacera).* The prepared AgNPs were characterized by using different analytical tools. UV–visible spectra were recorded, which exhibited a sharp surface plasmonic resonance (SPR) band at 430 nm and confirmed the formation of AgNPs. The spherical morphology of synthesized AgNPs was determined with the help of field emission scanning electron microscopy (FE-SEM) and transmission electron microscopy (TEM), and the average particle size was calculated using TEM and found to be 12.52 nm. The Fourier transformed infrared (FT-IR) spectrum of AgNPs showed characteristic bands of functional groups present in the biomolecules adsorb onto AgNPs, acting as a stabilizing agent. The crystallite nature of AgNPs formed was confirmed by the powder X-ray diffraction (PXRD) technique. The anticancerous activity of synthesized AgNPs was investigated against adherent human lung carcinoma cell A549. The minimal inhibition concentration (IC_{50} or MIC) value was found to be ~ 20 µg/mL for human lung carcinoma cell A549, and the result so obtained suggests that synthesized AgNPs via *B. lacera* possess a good ability to be used as an eco-friendly anticancerous agent. Moreover, the synthesized AgNPs possess good antioxidant activity compared to *B. lacera* plant leaves. The minimal inhibition concentration (IC_{50}) of ~ 6 µg/mL for synthesized AgNPs was found.

✉ Joy Sarkar
dr.joysarkar4@gmail.com

[1] Department of Chemistry, Lucknow University, Lucknow, Uttar Pradesh 226007, India

[2] Plant Diversity Systematics and Herbarium Division, CSIR-National Botanical Research Institute, Lucknow, Uttar Pradesh 226001, India

[3] Molecular and Human Genetics Laboratory, Department of Zoology, University of Lucknow, Lucknow 226007, India

[4] Department of Chemistry, B.S.N.V.P.G. College, Lucknow, Uttar Pradesh 226001, India

Graphical abstract

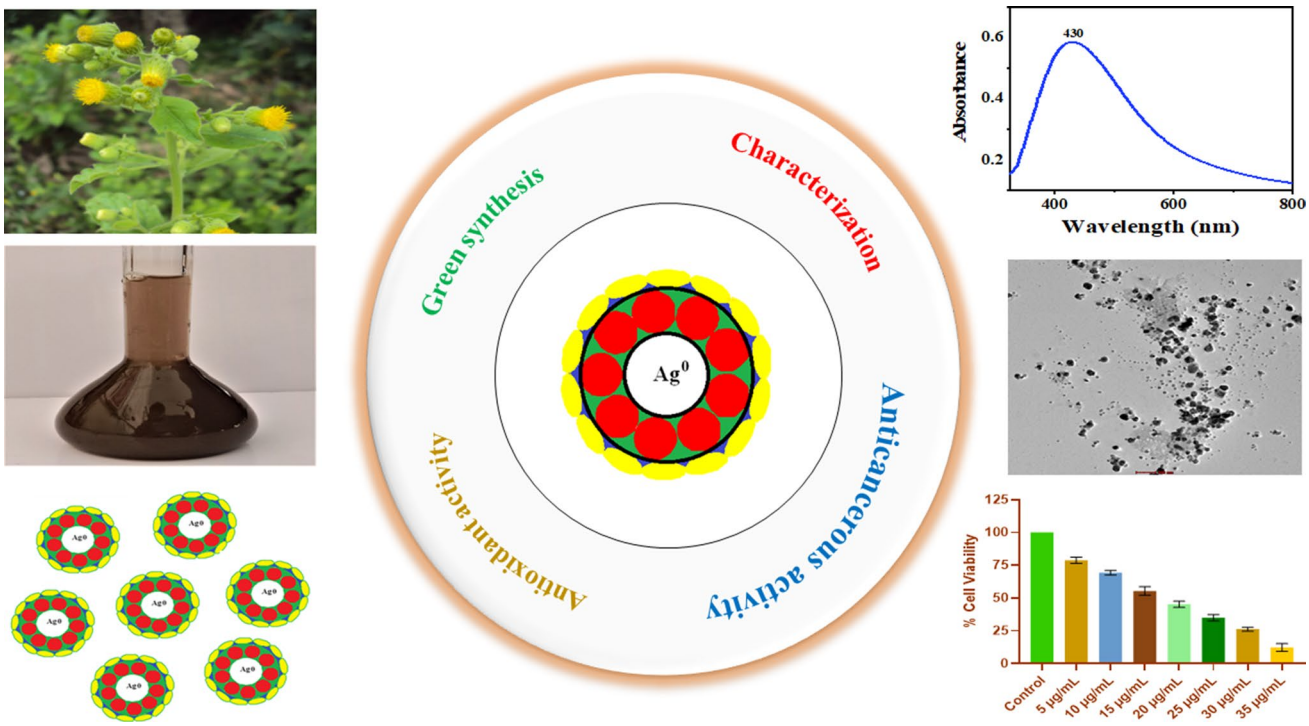

Keywords Silver nanoparticles · Green synthesis · *Blumea lacera* · Anticancerous activity · DPPH assay

Abbreviations

AgNPs	Silver nanoparticles
NPs	Nanoparticles
B. lacera	Blumea lacera
Fig.	Figure
FT-IR	Fourier transformed infrared
UV–Vis	Ultraviolet–visible
FE-SEM	Field emission scanning electron microscopy
DLS	Dynamic light scattering
EDX	Energy-dispersive X-ray spectroscopy
TEM	Transmission electron microscopy
PXRD	Powder X-ray diffraction
Eq.	Equation
MTT	3-(4,5-Dimethylthiazol-2-yl)-2,5- diphenyltetrazolium bromide tetrazolium salt
DPPH	2,2-Diphenylpicryl-1-hydrazyl
SPR	Surface plasmon resonance

Introduction

Over the last few decades, researchers have focused more on the green synthesis of plant-based metal nanoparticles (NPs) involving bio-organic frameworks as reducing and stabilizing agents (AlNadhari et al. 2020) since nature is the largest chemical laboratory with so many chemicals and plants are the richest source of organic and inorganic molecules generally called biomolecules. These biomolecules are isolated from plants and effectively used in the treatment of various diseases (Sharma et al. 2015). Green synthesis is a class of eco-friendly, cost-effective, and biocompatible approaches. It has many advantages over conventional methods (Sreelekha et al. 2021). Therefore, the present study attempts to provide a sustainable approach by involving the medicinal plant *Blumea lacera* (*B. lacera).* It exhibited excellent antimicrobial, cytotoxic, and antioxidant properties. The main chemical components present in *B. lacera* are campesterol, triterpenoid, and prenylated phenol glycoside, respectively. However, a few other biomolecules such as flavonoids and monoterpene glycosides are also found in them. The essential oil of *B. lacera* includes β-caryophyllene, thymol, hydroquinone, dimethyl ether, caryophyllene oxide, humulene, E-β-farnesene, and coniferal alcohol derivative (Mendhulkar et al. 2016; Ahmed et al. 2014).

Genus *B. lacera* is a wild plant found in Asia's tropical and sub-tropical zones, especially the Indian Subcontinent and Southeast Asia. *B. lacera* belongs to the family Asteraceae, and this family is one of the largest dicot families. It has a strong odor of terpentien, and its leaves are elliptical oblong or obovate shape. This plant is used in folk medicine

to treat cough, bronchitis, dysentery, and wound healing. In Ayurveda, it is described as an anthelmintic, thermogenic, anti-inflammatory, liver tonic, expectorant, ophthalmic, digestive, antipyretic, and memory enhancer. Conclusively, *B. lacera* is biomolecules-rich plant and it can act as a reducing as well as a stabilizing agent for the synthesis of NPs.

Nanoparticles with a wide class of nanotechnology contain particulate substances with at least one dimension less than 100 nm (Yaseen et al. 2022). NPs possess unique physiochemical properties such as electrical (Htwe et al. 2022), thermal (Braga et al. 2018), and optical (Mamdouh et al. 2022; Badán et al. 2020) properties due to higher surface-to-volume ratio, changes in specific characteristics such as size, shape, and morphology of particles, high diffusion rate, feasibility at lower temperatures, etc. (Gangwar et al. 2022). Also, it has been reported by many researchers that the noble metal-based NPs have a wide range of applications in biomedicals (Wu et al. 2012), food industry (Lugani et al. 2021), environmental remediation (Kumar et al 2022a, b), biosensing (Shen et al. 2013), cosmetics (Pulit-Prociak et al. 2019), pharmaceuticals (Hussein et al. 2021), nanomedicines (Yaseen et al. 2022), etc., After performing extensive literature survey, silver nanoparticles (AgNPs) were found to have potential applications in almost wide areas of research such as biomedical, catalysis, food industries, environmental remediation, biosensing, water purification, and so on. Nonetheless, AgNPs are also known to possess excellent antimicrobial and antioxidant properties (Gangwar et al. 2022). Since nanobiotechnology is a rapidly growing field and played an essential role in the biomedical field for disease diagnosis, treatment, and curation (Shahcheraghi et al 2022). In the present scenario, cancer has become a serious issue. However, several therapeutic modes, i.e., chemical and physical therapies, are well known to overcome this problem. Since the drug dose and high irradiation of the source during therapy may cause bad effects on the normal cells, conventional methods of cancer treatment such as surgery, radiotherapy, and chemotherapy have several limitations related to drug toxicity, lack of specificity, unpredictable drug side effects, and drug resistance problems (Ratan et al. 2020). To overlay these problems, metal-based NPs are more popular among researchers and also, capable of enhancing the efficiency of cancer therapy (Gangwar et al. 2022). In this investigation, an attempt has been made to evaluate cytotoxic activity against the lung cancer cell (cell lines A549) of synthesized AgNPs using *B. lacera* leaf extract for the very first time. The antioxidant activity of *B. lacera* leaf extract was reported (Ahmed et al. 2014), but the antioxidant activity of AgNPs synthesized by using *B. lacer* using DPPH (2,2-diphenylpicryl-1-hydrazyl) is still not known.

Therefore, the main aim of the present study is to provide a method for the synthesis of AgNPs using *B. lacera* leaf extract. The synthesized AgNPs were characterized with the help of different analytical techniques such as UV–visible spectroscopy (UV–Vis), dynamic light scattering (DLS), Fourier transformed Infrared (FT-IR) spectroscopy, field emission scanning electron microscopy (FE-SEM), transmission electron microscopy (TEM), energy-dispersive X-ray spectroscopy (EDX), and powder X-ray diffraction (PXRD). Lastly, the evaluation of the antioxidant activity and cytotoxicity of the AgNPs was performed to employ them as potential material for biomedical applications. It also provides a comparative study of antioxidant activities between the medicinal plant *B. lacera* leaf extract and synthesized AgNPs. Consequently, it is observed that AgNPs show more antioxidant activity as compared to leaf extract of *B. lacera.* Until now, the cytotoxic activity of AgNPs using *B. lacera* at pH 9.0 against adherent human lung carcinoma cells (A459) is unknown. The comparison of biosynthesized AgNPs anticancerous activity against human lung carcinoma cell A549 and DPPH antioxidant antioxidant activity is provided in Table 1.

Experimental

Materials

All reagents and chemicals used in the present investigation were of analytical grades. Silver nitrate ($AgNO_3$, 99.90%) (E Merck Ltd., Mumbai, India) and sodium hydroxide (NaOH, 99%) (S D fines chemicals Ltd., Mumbai, India) were used as received. For anticancerous activity, Dulbecco's modified Eagle medium (DMEM), trypan blue, 0.25% trypsin–EDTA solution, fetal bovine serum (FBS), antibiotic–antimycotic (Ab/Am) solution, 3-(4,5-dimethylthiazol-2-yl)-2,5-diphenyltetrazolium bromide tetrazolium salt (MTT), and phosphate buffered saline (PBS) were used. For antioxidant activity, (2,2-diphenylpicryl-1-hydrazyl) (DPPH) was used as received.

Methods

Preparation of *B. Lacera* leaf extract

The plant was authenticated (herbarium number 330351) by Plant Diversity Systematics and Herbarium Division, CSIR-National Botanical Research Institute, Lucknow-226001, Uttar Pradesh, India. The leaf of the medicinal plant *B. lacera* was first rinsed with tap water and then doubled-distilled water to remove all dust particles. The leaves were chopped to approximately 3–4 mm and used as starting biomass. The fresh materials (25 g) biomass was boiled with double-distilled water (250 mL) at 40 °C in a beaker and reduced the volume to its half. The mixture was cooled and filtered successively through Whatman filter paper no. 42. Finally,

Table 1 Comparison of biosynthesized AgNPs anticancerous activity against human lung carcinoma cell A549 and DPPH antioxidant activity

Plants	Part used	Size (nm)/morphology	Anticancerous activity (IC_{50}) values for human lung carcinoma cell A549 (in vitro)	(DPPH) Antioxidant activity (IC_{50}) values	References
Cymodocea serrulata	Leaf	5–25/spherical	100 µg/mL	–	Paaniappan et al. (2015)
Origanum vulgare	Leaf	63–85/Spherical	100 µg/mL	–	Sankar et al. (2013)
Syzygium samarangense	Leaf	–/Spherical	87.37 µg/mL	–	Thampi et al. (2015)
Rosa damascena	Petal	84/ Spherical	80 µg/mL	–	Venkatesan et al. (2014)
Momordica charantia	Fruit	1–40/Spherical	51.93 µg/mL	–	Jha et al. (2018)
Allium sativum	Root	15–35/Spherical	22 µg/mL	–	Padmini et al. (2022)
Atrocarpus altilis	Leaf	10–40/ spherical	–	51.17 µg/mL	Ravichandran et al. (2016)
Hypericum perforatum	Leaf	20–50/spherical	–	35.88 µg/mL	Alahmad et al. (2021)
Green tea	Leaf	5–30/spherical	17 µg/mL	7.74 µg/mL	Selvan et al. (2018)
Garlic leaf extract	Leaf	5–30/spherical	13 µg/mL	6.89 µg/mL	Selvan et al. (2018)
Turmeric powder	Root	5–30/spherical	11 µg/mL	6.03 µg/mL	Selvan et al. (2018)
B. lacera	Leaf	10–30/spherical	20 µg/mL	6 µg/mL	This work

the leaf extract was stored at 4 °C for further use in the synthesis of AgNPs and other experimental studies (Ameen et al. 2019; Garibo et al. 2020).

Biosynthesis of AgNPs

Silver nanoparticle synthesis was carried out as described by Jadhav et al. (2018, 2016). Briefly, the preparation of AgNPs was achieved under optimized conditions, by mixing 3 mL of *B. lacera* plant leaf extract and 7 mL 1×10^{-3} M $AgNO_3$ at pH = 9.0, followed by 3-h continuous stirring at a speed of 620 rounds per minute at room temperature. The color change from light brown to dark brown indicated the formation of the AgNPs (Fig. 1), at 430 nm surface plasmon resonance (SPR) band. Further, the prepared AgNPs were purified by subjecting it to high-speed refrigerated centrifugation (Eppendorf 5810 R) at 13,000 rpm maintained 4 °C for 30 min. The AgNPs were obtained after the decantation of the supernatant liquid. The prepared AgNPs were washed several times with double-distilled water and finally with 0.01% acetic acid (0.01 mL acetic acid present in 100 mL of double-distilled water) to eliminate the contamination from the residue of AgNPs. Finally, AgNPs were lyophilized with the help of CT 60e (HETO) and stored in an airtight ampule at 4 °C for further use.

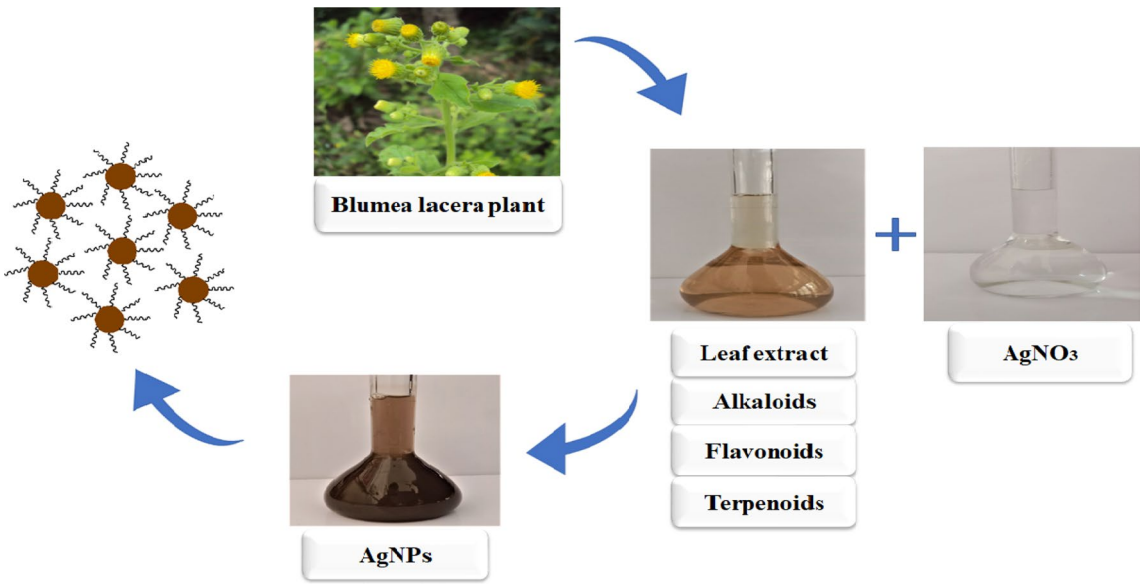

Fig. 1 Schematic representation for the synthesis of silver nanoparticles by using the medicinal plant *Blumea lacera* leaf extract

Instrumentation

The pH of the samples was measured with an automated digital pH meter (μpH meter 361 Systronic, India). The formation AgNPs were initially screened by UV–visible double-beam spectrophotometer (A Lab UV next-generation) to record absorption spectra. For the confirmation of the functional groups involved in the synthesis of AgNPs, FT-IR (Thermoscientific Nicole 6700) was used. A rotating anode X-ray diffractometer apparatus (Rigaku, Smart lab 9 kW, rotating anode X-ray diffractometer) was used to confirm the crystallographic structure of the AgNPs using Cu-K_α X-ray of wavelength 1.540A° in the range of 2θ equal to 30° to 80° was used to the phase structure. For visualization the morphology and to record the EDX profile of the synthesized AgNPs was observed on FE-SEM (JEOL JSM 7610f). For morphology, images are also captured on a transmission electron microscope (TEM, Talos machine operating at 200 kV). For hydrodynamic size and zeta potential, dynamic light scattering (DLS, Zetasizer Nano of Malvern Instruments, Worcestershire, UK) was used.

Anticancer activity

Cell viability A549 cells (ATCC, Rockville, Manasotas, VA, USA) were grown in DMEM supplemented with 2 mM L-glutamine and 10% v/v fetal bovine serum (FBS) and placed in a CO_2 incubator at 37^0C in a humidified environment with 5% CO_2 (Yadav et al. 2021). After the cells reached 80% confluency, PBS was used to wash the cells, followed by trypsinization with the trypsin–EDTA solution and the addition of the culture media. For the next studies, the cells were exposed after being seeded in a culture plate for 24 h.

MTT assay The anticancer activity of AgNPs was tested on the A549 cells (Singh et al. 2020). AgNPs were dissolved in PBS and further diluted as per requirement. Cell viability of control and treated cells was assessed by 3-(4,5- dimethylthiazol-2-yl)-2,5-diphenyltetrazolium bromide dye (MTT; Himedia, USA) reduction assay as described by Mosmann (1983). The cells were seeded at the density of 1×10^4 cells/well in 96-well plate; after the incubation period, cells were treated with different concentrations (5 to 35 μg/mL) of AgNPs and grown in CO_2 incubator for 24 h. After the treatment period, 10 μL of MTT (0.5 mg/mL) was added to each well and incubated at 37 °C for 4 h. Thereafter, medium was removed and added 100 μL of DMSO and then incubated for 15 min at room temperature. The plate was read at 540 nm, and percent cell viability was calculated and statistically analyzed using GraphPad Prism (Gangwar et al. 2023).

Antioxidant activity

To evaluate antioxidant activity, DPPH assay has been used. All test solutions and stock solution (DPPH; 0.254 mM) were prepared in ethyl alcohol. To each test solution of *B. lacera* leaf extract or AgNPs of concentrations 2, 4, 6, 8, and10 μg/mL, stock solution of DPPH (1.5 mL) was added. Test solutions were incubated for an hour at room temperature and subject to record the absorption spectra at 516 nm. Similarly, the absorption spectra of the test solutions were recorded after incubation of 24, 48, and 72 h.

Results and discussion

Phytochemical analysis of *B. lacera* leaf extract

Medicinal plant leaf extracts of *B. lacera* contain different types of phytochemicals with huge therapeutic values. As compared with a synthetic drug, the green synthesized drug is considered safe and natural. For analysis of phytoconstituents, various chemical tests were performed with five different extracts [water extract (WE), methanol extract (ME), acetone extract (AE), chloroform extract (CE) and petroleum ether extract (PEE)] of *B. lacera* and given in Table 2.

Table 2 List of phytochemicals of *B. lacera* leaf extract

S. No	Phytochemical	Test performed	WE	ME	AE	CE	PEE
1	Phenol/ Tannins	Ferric Chloride test	+	+	+	−	+
2	Steroids	Ring test	−	+	+	−	+
3	Carbohydrates	Molish test	−	+	−	−	−
4	Protein	Biuret test	+	+	+	−	+
5	Flavonoids	Ethyl acetate test	+	+	+	+	−
6	Saponins	Foam test	−	+	−	+	−
7	Glycosides	Legal test	−	−	−	−	−
8	Terpenoids	Salkowski test	+	+	−	−	−
9	Alkaloids	Mayer test	−	+	+	−	+

+ indicates = Presence, − indicates = Absence

Characterization of AgNPs

Green-synthesized silver nanoparticles by using *B. lacera* plant extract were characterized by using UV–Vis spectrophotometer, TEM, and DLS analysis in colloidal form and FT-IR, PXRD, FE-SEM, EDX analysis in powder form of AgNPs, respectively.

UV–visible analysis and optical bandgap evaluation

The surface plasmon resonance (SPR) band of the NPs are strongly affected by their morphology and size. Therefore, UV–visible spectrophotometry became an essential tool for the initial confirmation of AgNPs formation (Aziz et al 2017). The absorption spectra of *B. lacera* leaves extract contain one 325 nm (Fig. 2a). The formation of AgNPs indicated a change in color from light brown to dark brown which intensified with time. This change in the color of the solution was confirmed by UV–visible spectrophotometer, giving a strong SPR band at 430 nm, (Fig. 2b), which was also confirmed by a researcher (Khalir et al. 2020). The intensity of the peak increases with time (overlay spectra of reaction mixture) is also represented in (Fig. 2c). The band at 430 nm intensifies with time indicating that the synthesis of AgNPs has narrow particle size distribution. Moreover, the optical properties of synthesized AgNPs were observed with the help of absorption spectra recorded in the range of 325–800 nm. The optical band gap was calculated using Tauc relationship ($\alpha = (\frac{k}{h\nu})(h\nu\text{-Eg})^n$) (Gangwar et al. 2022) where α is the absorbance coefficient, k is a constant, hν is the photon energy, h is the Plank's constant, Eg is the band gap, and n is the number that describes the electronic transitions between valance band and conduction band. The value of absorbance coefficient (α) is calculated with the help of absorbance and thickness of the cuvette (t) using the formula $\alpha = 2.303A/t$, and the optical band gap can be obtained by plotting a graph between $(\alpha h\nu)^2$ (in $(\text{eV cm}^{-1})^2$) and energy (hν in eV). The linear portion of the curve obtained at higher energy on extrapolation toward the energy axis where $\alpha = 0$ gives the optical band gaps of synthesized AgNPs (Fig. 2d). The optical band gap (Eg) of AgNPs determined with the help of the plot is 2.10 eV. This result is in good agreement with the result obtained by Mistry et al. (2020).

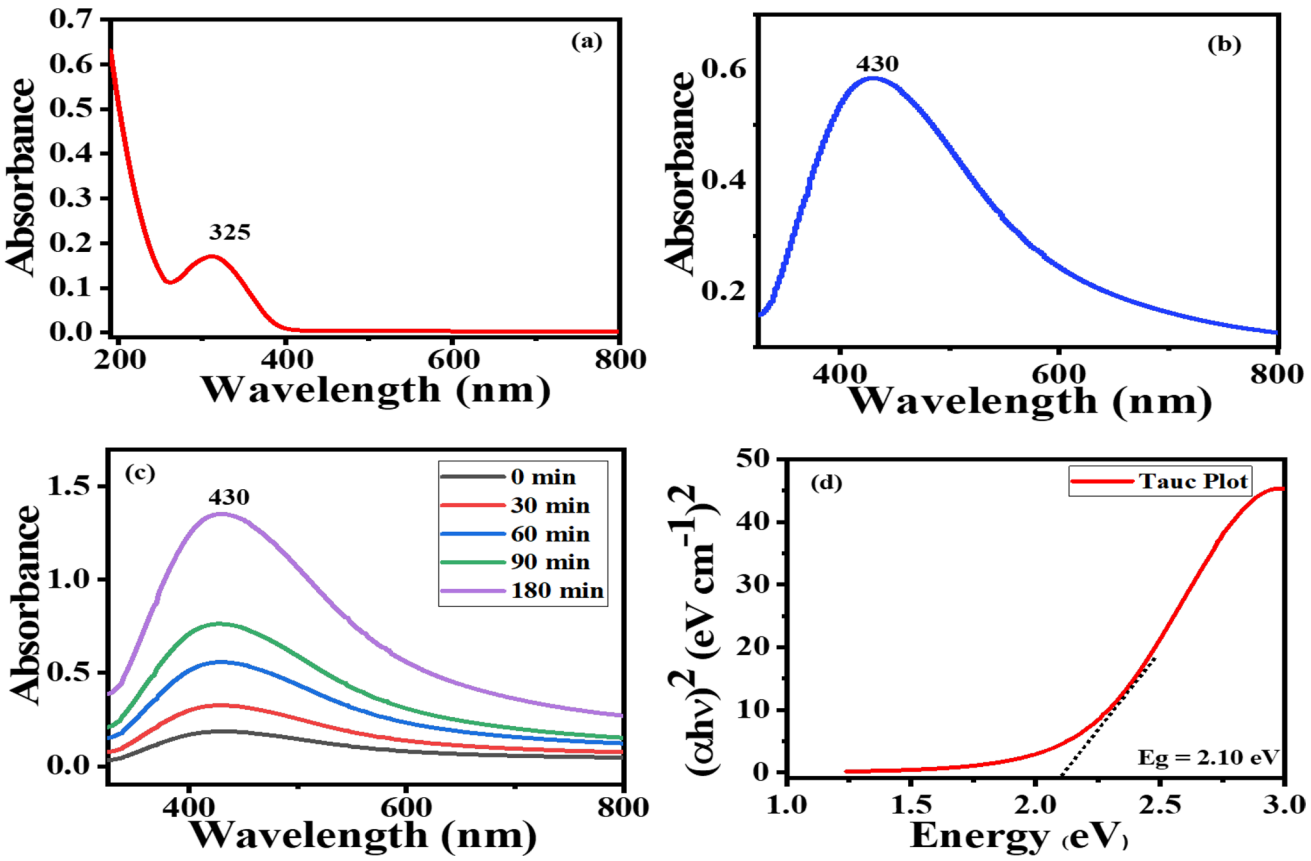

Fig. 2 **a** UV–visible spectra of leaf extract *B. lacera in aqueous medium* **b** UV–visible spectra of synthesized silver nanoparticles by using leaf extract of *B. lacera*, **c** Change in the value of absorption with time when 7 mL of 1×10^{-3} M silver nitrate solution mixed with 3 mL leaf extract *B. lacera* (overlay spectra of reaction mixture) and **d** optical band gap (Eg = 2.10 eV) of synthesized AgNPs

FT-IR analysis

FT-IR spectra of synthesized AgNPs were recorded from wavenumber 3725–350 cm^{-1} (Fig. 3). FT-IR analysis provides evidence that the phytochemicals such as alkaloids, flavonoids, triterpenoids, amino acids, proteins, polyphenols, etc., worked as both capping and stabilizing agent. FT-IR band centered at 3483 cm^{-1} is due to –OH, –NH stretching vibration. Two weak bands were obtained at 2911 and 2327 cm^{-1} corresponding to C–H stretching frequency of the aliphatic methylene group and the overtone of the C–H bending of the aromatic fragment, respectively. A band at 1820 and 1636 cm^{-1} is due to C=O stretching vibration of carbonyl compounds. A band at 1535 cm^{-1} was observed because of the stretching of the sp^2 hybridized carbon–carbon double bond of the aromatic fragment. A band at 1387 cm^{-1} corresponding to the –C–O group was observed. A band at 1083 cm^{-1} was observed due to the C–H group of rings stretching or in-plane bending. There are three bands at the lower region below 1000 cm^{-1} observed due to silver metal's inter-atomic absorption vibration (Gangwar et al. 2022; Sytu et al. 2018). Therefore, from the FT-IR analysis, it may be concluded that, AgNPs present in an aqueous medium is stabilized in colloidal form by these different functional groups attached to the phytochemicals. Hence, these functional groups work as reducing as well as stabilizing agents (Kumar et al. 2022a, b).

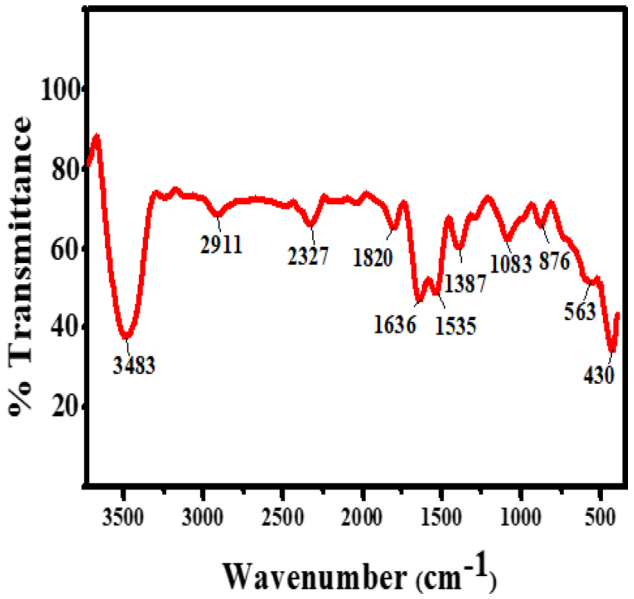

Fig. 3 FT-IR spectrum of synthesized silver nanoparticles by using *B. lacera* leaf extract. This FT-IR spectrum shows different functional groups of phytochemicals which are attached to the surface of silver nanoparticles as a capping agent

PXRD analysis

To confirm the presence of crystalline silver in the synthesized AgNPs by *B. lacera* leaf extract, powder X-ray diffraction (PXRD) was obtained (Fig. 4a). The PXRD pattern of the synthesized AgNPs shows several peaks, in which five peaks more prominently located at 38.16°, 44.28°, 64.54°, 77.46°, and 81.58° 2θ values are analogous to the (1 1 1), (2 0 0), (2 2 0), (3 1 1) and (2 2 2) hkl planes, respectively (Anandalakshmi et al. 2016) with best similarities with Joint Committee on Powder Diffraction standards (JCPDS) file no. 04–0783 (Gangwar et al. 2021). PXRD confirms that the reduction of silver ions and the resulting nanoparticles correspond to the face-centered cubic structure (FCC) of silver nanoparticles (Karthik et al. 2015; Mishra et al. 2021; Shalini et al 2022). The peak corresponding plane (111) at 38.16° is the most intense than other peaks, suggesting that the AgNPs are fine and small. The large peak indicates that

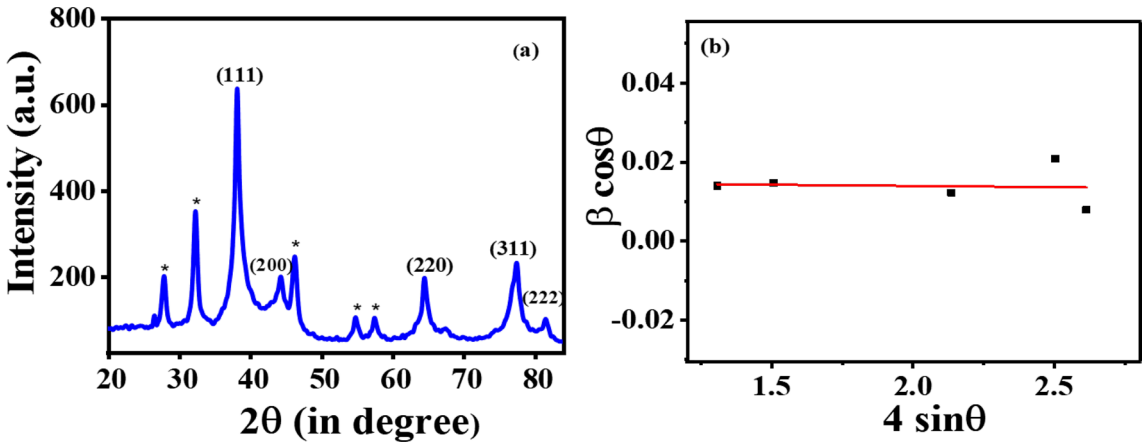

Fig. 4 **a** X- ray diffraction (XRD) pattern for silver nanoparticles synthesized by *B. lacera* leaf extract and **b** Williamson -Hall plot for synthesized silver nanoparticles

the crystal-sized particles are in the nanoscale (Gangwar et al. 2021).

In addition, some peaks that are obvious (marked as *) in the PXRD at 27.86°, 32.28°, 46.26°, 54.84° and 57.50° could be attributed to metabolite capping the AgNPs (Labulo et al. 2022; Anandalakshmi et al. 2016). The average crystalline size of AgNPs was found to be 10.96 nm, which was estimated using the Debye–Scherrer's equation, Eq. (1) (Gangwar et al. 2021). Equations 2–5 were used to evaluate different theoretical parameters related to the crystal.

$$D = 0.9\,\lambda / \beta \cos\theta \tag{1}$$

$$2d \sin\theta = n\lambda \tag{2}$$

$$\mathrm{dhkl} = a/\sqrt{h^2 + k^2 + l^2} \tag{3}$$

$$\beta \cos\theta = k\lambda / D + 4\varepsilon \sin\theta \tag{4}$$

$$\delta = 1/D^2 \tag{5}$$

Here, in the above equations the different abbreviation used are given as under. D is the crystallite size, λ is the wavelength of X-ray radiation (λ = 1.540 A^0), β is the full width at half maxima (FWHM) of the respective peak, θ is the diffraction angle, d is the interplanar spacing between two successive planes in a family (h k l) and it is commonly indicated as d_{hkl}, "a" is the lattice parameter, 'k' is Scherrer constant, ε is the strain, and δ is dislocation density. The theoretical parameters obtained with the help of PXRD data are provided in Table 3. The value of d-spacing can be calculated using Bragg's law represented in Eq. (2). The lattice parameter "a" can be calculated by Eq. (3), and the mean value of the lattice parameter of AgNPs is 4.076 A°.

The broadness in the diffraction peak is due to the very small crystallite size and strain in the synthesized nanoparticles. For calculating the accurate crystallite size of AgNPs, the Williamson–Hall (W–H) plot, between β cosθ on the y-axis and 4 sinθ on the x-axis, was represented as shown in (Fig. 4b) using Eq. (4), and this plot gives a straight line with slope ε, which gives strain, and intercept is equal to kλ/D. The value of strain from the W–H plot was calculated at 6.246×10^{-4}, and the average crystallite size was 9.122 nm. The value of slope (ε) is negative which shows that AgNPs are compressive in nature [22]. The crystallite size of AgNPs is small, has more dislocation density, and hence harder material. The value of dislocation density from Eq. (5) is found to be 12.017×10^{15} m^{-2}. The crystalline index (CI or Icry) of synthesized nanoparticles is calculated by taking the ratio of average particle size obtained by TEM analysis to the average crystalline size obtained by PXRD analysis, and it is found to be 1.37, which shows the monocrystalline nature of AgNPs.

FE-SEM analysis

Preliminary surface morphological and nanostructural studies of synthesized AgNPs were done by using FE-SEM analyses. FE-SEM images at 100 nm, a and b with different magnification (×30,000) and (×50,000), taken respectively (Fig. 5). Before analysis, a carbon-coated copper grid was prepared and then AgNPs were coated with conducting material Pd–Pt alloy: substrate is represented in images, which indicate the sample has diversity in the surface morphology. For low-magnification images show, the non-spherical and quasi-spherical surface morphology of synthesized AgNPs, with little agglomeration in the solid phase.

TEM analysis

To know more clearly about the morphology and particle size of synthesized AgNPs, TEM analysis was performed. TEM images were captured at two different scales 100 nm and 50 nm (Fig. 6a, b). From the images, it can be observed that most of the AgNPs have spherical morphology which matches well with the FE-SEM result. It is quite clear from the TEM images that the prepared nanoparticles are polydispersive in nature which matches well with the PDI 0.759 estimated using the DLS technique. A histogram was drawn after measuring the diameter of nanoparticles from the TEM image to calculate their average diameter and given in (Fig. 6c), and Gaussian distribution plot was also obtained by measuring AgNPs by TEM image at 100 nm

Table 3 List of theoretical parameters obtained from XRD Data

2θ (degree)	(hkl)	FWHM (β) (radian)	Crystalline size (D) (nm)	Spacing (d) (nm)	Lattice parameter (a) (A^0)
38.16	(111)	0.0148	9.913	0.236	4.08
44.28	(200)	0.0159	9.429	0.204	4.08
64.54	(220)	0.0145	11.333	0.144	4.07
77.46	(311)	0.0267	6.659	0.123	4.07
81.58	(222)	0.0104	17.49	0.118	4.08

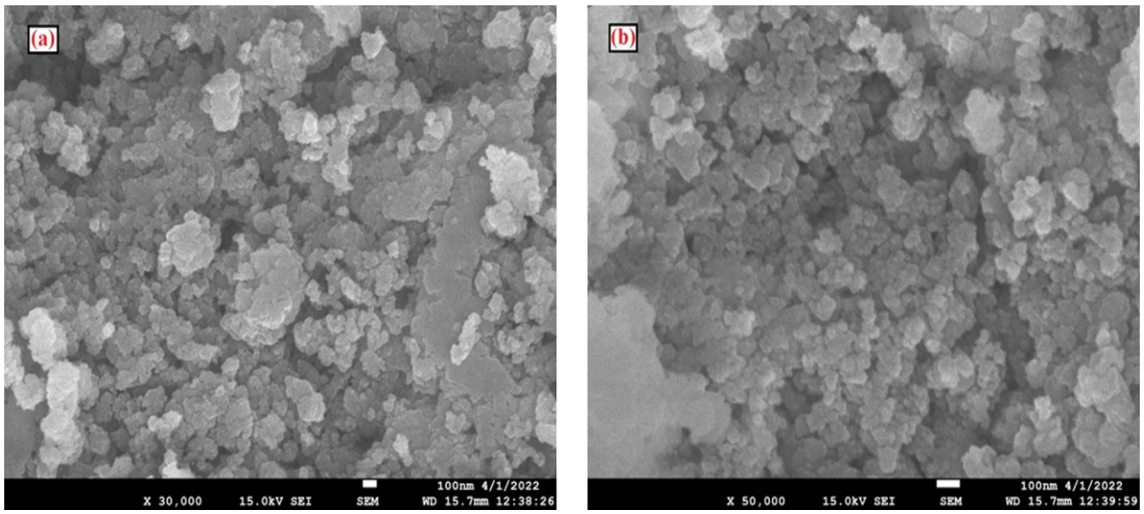

Fig. 5 FE-SEM images of AgNPs at a 100 nm scale with two different magnifications **a** at 30,000 and **b** at 50,000

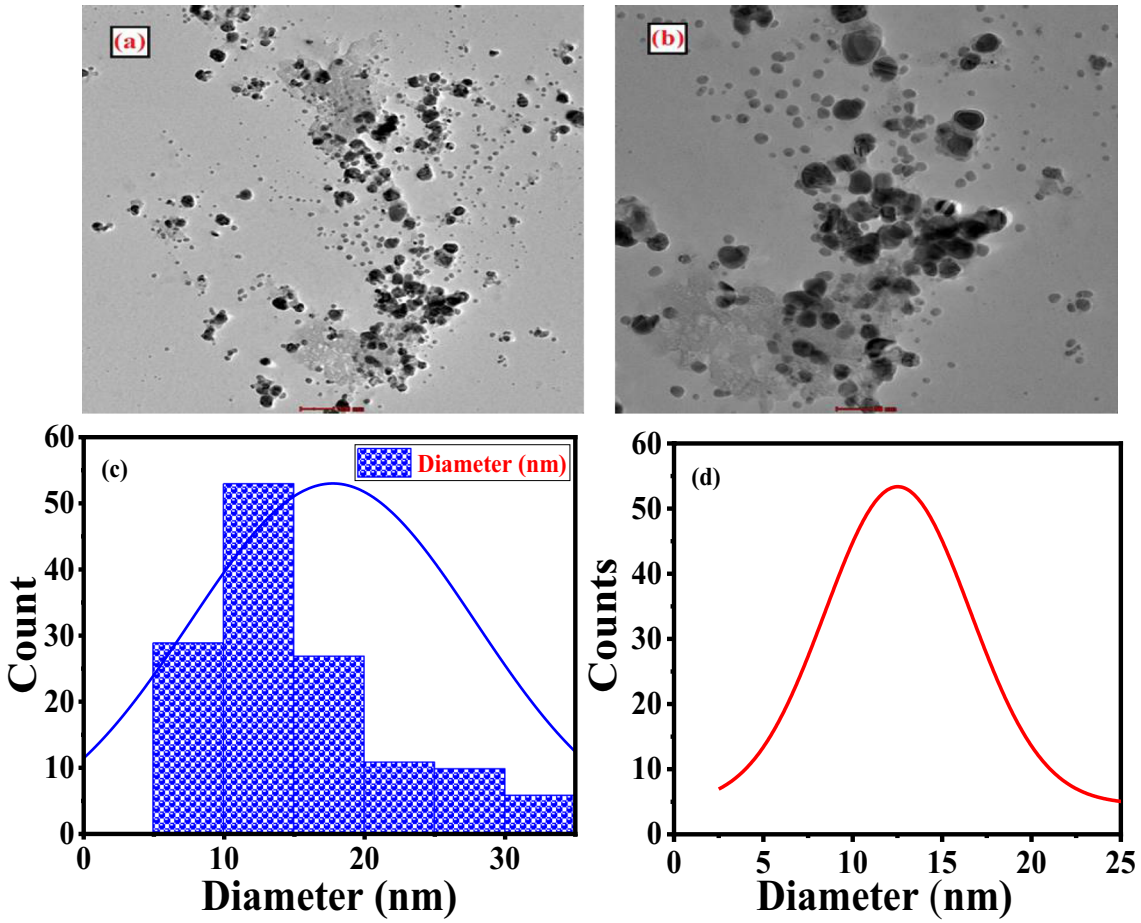

Fig. 6 TEM images of AgNPs at two different scales **a** 100 nm and **b** 50 nm **c** Histogram analysis and **d** Gaussian distribution plot obtained by measurement AgNPs by TEM image at 100 nm. The average diameter of synthesized silver nanoparticles was found to be 12.52 nm

and provided in (Fig. 6d). However, the average diameter of AgNPs is 12.52 nm having the standard error of 0.42 units which is close to the W–H plot result (Shalini et al 2022; Zhu et al. 2022).

EDX analysis

EDX analysis was performed to get the exact elemental composition of each element present in the sample. It also determines the homogeneity and to confirm the formation of AgNPs from silver ions. In the EDX profile, a signal nearly at 3.00 keV was obtained which shows formation of silver nanoparticles. Along with these, two more peaks nearly at 0.50 keV were also observed for carbon and oxygen represented in (Fig. 7a). The percentage weight composition for each element is also represented in the form of 3D clustered cone and shown in (Fig. 7b). (Calderón-Jiménez et al. 2022; Xu et al. 2020).

DLS analysis

Dynamic light scattering (DLS) is a crucial technique used for the analysis of the hydrodynamic size and zeta potential (ZP) or electrokinetic potential of the AgNPs colloids. The green synthesis of AgNPs involves a metal core and capping of biomolecules on the surface of the metal core to stabilize it (Guilger-Casagrande et al. 2021). The size distribution of AgNPs colloid is represented in (Fig. 8a). The hydrodynamic size observed for AgNPs colloid is 94.50 nm having a polydispersity index (PDI) of 0.759 which shows the polydisperse nature of the synthesized silver nanoparticles. This polydispersity nature was also confirmed by the TEM images and Gaussian distribution plot. The zeta potential is an important parameter that gives an idea about the stability of AgNPs by evaluation of surface charge shown in (Fig. 8b) (Khatoon et al. 2017). The zeta potential of synthesized AgNPs was observed at -10.5 mV which represents negative charge distribution over the AgNPs colloids. The stability of AgNPs colloids increases with an increased negative charge over the synthesized nanoparticles (Jagwani et al. 2020).

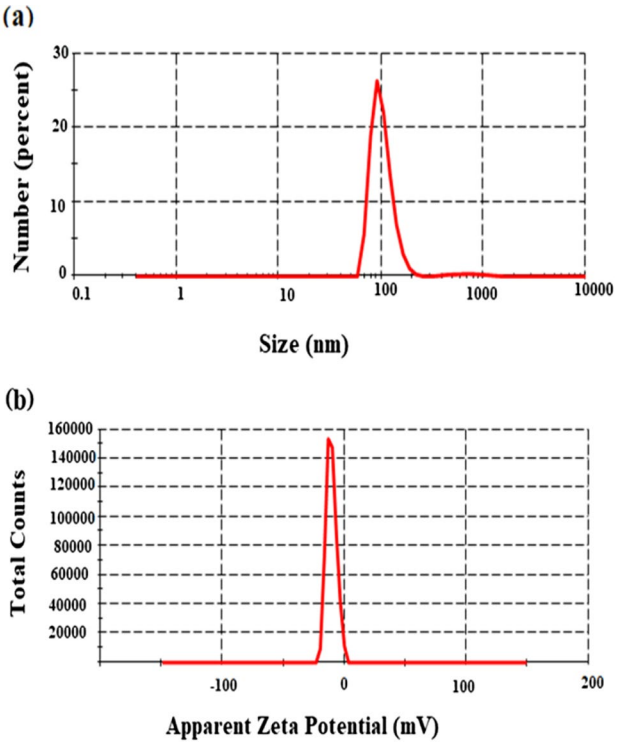

Fig. 8 DLS analysis of AgNPs **a** Size distribution plot. The hydrodynamic size observed for synthesized silver nanoparticles is 94.50 nm and **b** Zeta potential distribution plot

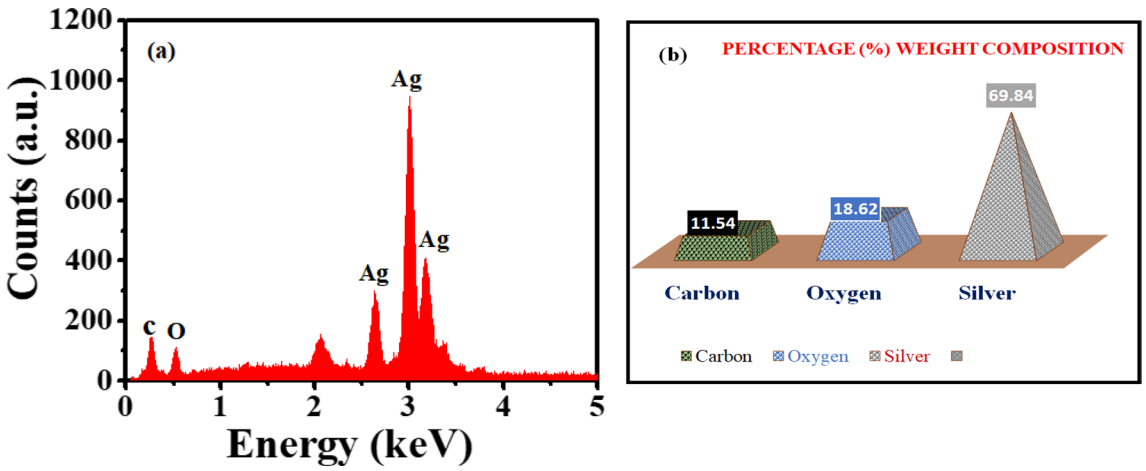

Fig. 7 **a** EDX profile of synthesized silver nanoparticles. The strong peak at 3.00 keV confirms the presence of silver and **b** 3D Clustered cone chart represent % weight composition of elements detected in EDX profile of silver nanoparticles

Anticancerous activity

Anticancer activity of AgNPs was assessed in terms of the percent cell viability at various concentrations. It was found that AgNPs had an IC_{50} value of ~ 20 µg/mL. Compared to 5 µg/mL, 35 µg/mL was shown to have a much higher toxicity level. Compared to the control group, the treated cells had significantly lower survivability. Therefore, from this, it can be predicted that the functional groups present in biomolecules involving the bio-organic framework of AgNPs are responsible for higher uptake via cell line A549 as compared to those stabilized by several stabilizers. A plot for % cell viability versus concentration is shown in (Fig. 9) (Mosmann 1983), and (Fig. 10) shows the morphology of A549 cells was altered after 24 h in cells containing various concentration of synthesized AgNPs. The percentage cell viability was calculated by using the formula, Eq. (6) (Gangwar et al. 2022; Kumar et al. 2022a, b).

$$\%\text{Cell viability} = \frac{[(\text{control absorbance}) - (\text{Test absorbance})]}{(\text{control absorbance})} \times 100 \quad (6)$$

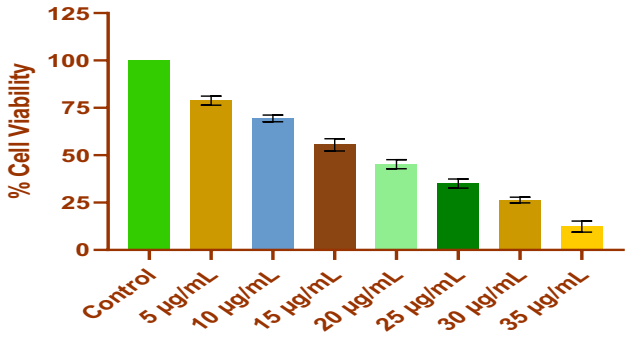

Fig. 9 Percent cell viability of A549 Cells treated with different concentrations of synthesized silver nanoparticles by using *B. lacera* leaf extract

Comparative study of antioxidant properties of *B. lacera* plant leaf extract and synthesized AgNPs

The DPPH shows absorption at 516 nm, as the free radicals of DPPH interact with a reducing agent leaf extract of *B. lacera* or with AgNPs, the absorbance intensity at 516 nm decreases, and the color of DPPH changes from purple to yellowish or colorless. The reaction of DPPH with AgNPs

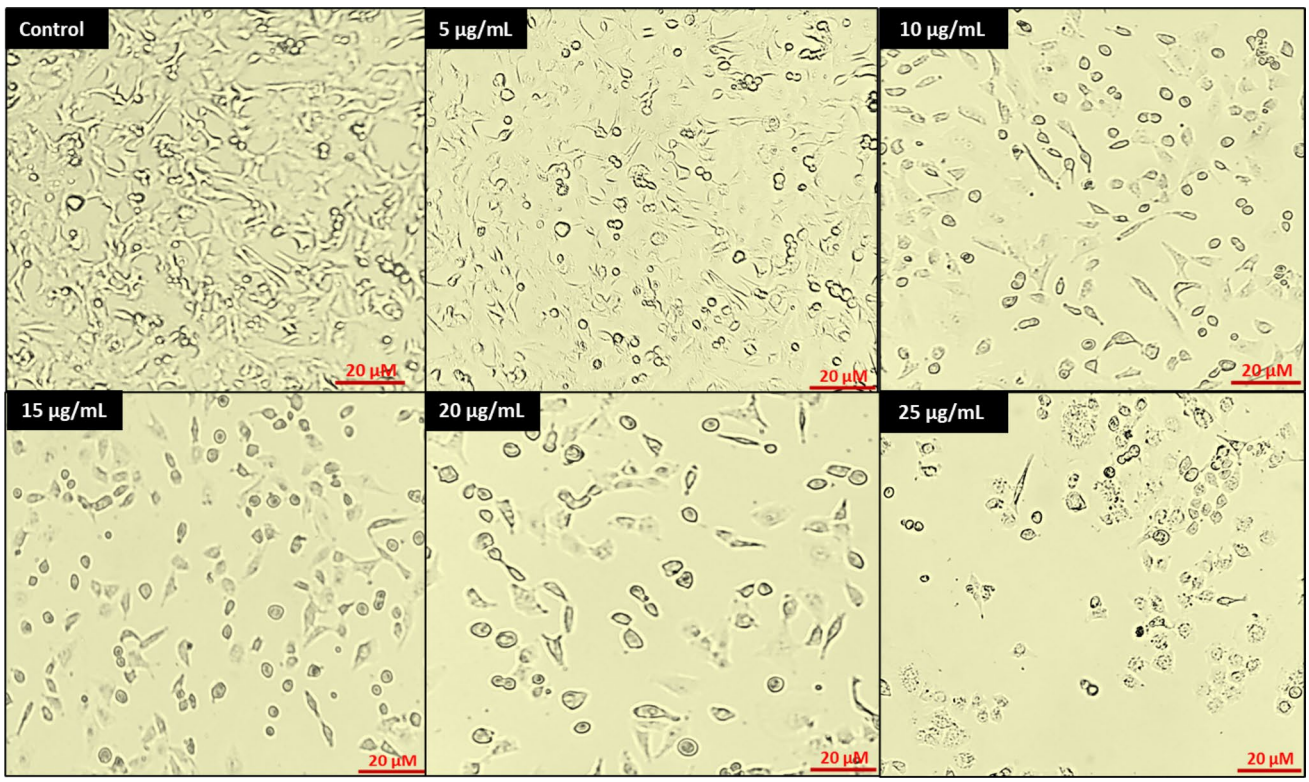

Fig. 10 Showing the morphology of A549 cells was altered after 24 h in cells containing various concentrations of synthesized silver nanoparticles by using *B. lacera* leaf extract. Exposed cells appeared more spherical in these areas and showed fewer cell–cell interactions than untreated cells in comparison to the control

Scheme 1 Mechanism of DPPH scavenging (A-H represents antioxidant)

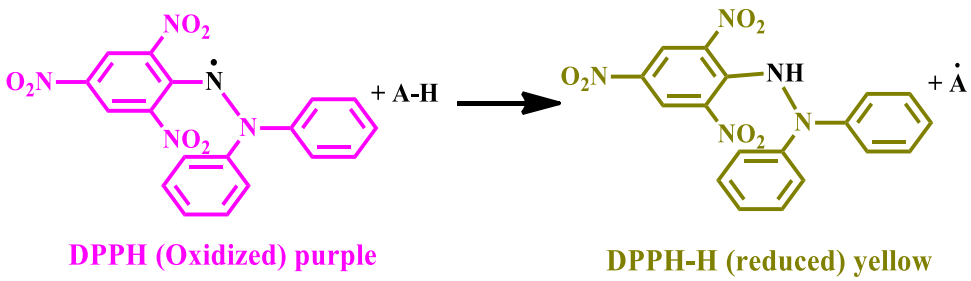

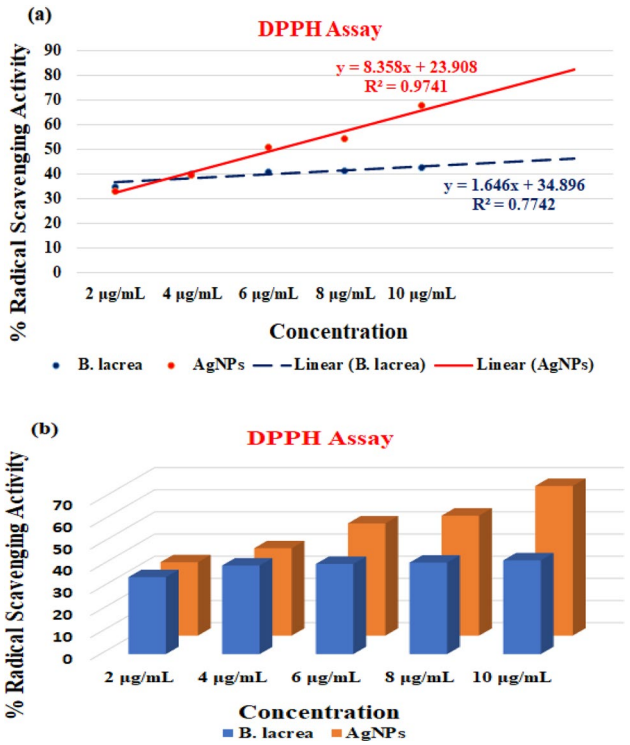

Fig. 11 Comparative antioxidant activity of *B. lacera* plant leaf extract and synthesized AgNPs at 72 h **a** Line graph and **b** Bar diagram

or leaf extract is shown in Scheme 1. This change in color or absorbance intensity depends upon the concentration of the reducing agent (Adewale et al. 2020; Sreelekha et al. 2021; Labulo et al. 2022).

The percent DPPH scavenging effect was calculated by using the following equation, Eq. (7).

$$\%\text{Inhibition} = \frac{\text{Absorption of control} - \text{Absorption of test}}{\text{Absorption of control}} \times 100 \quad (7)$$

The scavenging activity of both increases linearly with the increased concentration of leaf extract (or AgNPs) as shown in (Fig. 11a). The DPPH scavenging activity of *B. lacera* plant and synthesized AgNPs is shown in (Fig. 11b). It is clear from the graph that the AgNPs has more slope than *B. lacera*, which suggests that the AgNPs have more antioxidant properties than *B. lacera*. It is because more phenolic contents are attached to the surface of synthesized silver nanoparticles as a capping agent (Abdel-Aziz et al. 2013). It was observed that AgNPs had an IC_{50} of ~ 6 µg/mL which is more than *B. lacera*. The scavenging activity for the concentration of 10 µg/mL at 72 h was done both for green-synthesized AgNPs and for *B. lacera* leaf extract, and it was elucidated that the scavenging activity of AgNPs (67.56%) was far better than the plant extract (42.36%), and the calculated data are shown in Table 4. The results clearly suggest that the AgNPs have superior antioxidant activity compared to *B. lacer* (BalaKumaran et al. 2022). Conclusively, the combinatorial antioxidant activity is more effective than *B. lacera* plant leaf extract alone.

Table 4 Comparative study of Percentage radical scavenging of each set of *B. lacera* plant leaf extract and AgNPs, *Absorption of control* = *0.857*

Time of Incubation (hours)	% Radical scavenging									
	2 µg/mL		4 µg/mL		6 µg/mL		8 µg/mL		10 µg/mL	
	Plant	AgNPs	Plant	AgNPs	Plant	AgNPs	Plant	AgNPs	Plant	AgNPs
1	05.01	09.10	05.48	11.90	06.76	17.85	07.46	18.67	08.86	24.15
24	19.95	33.60	22.87	37.10	24.85	40.37	26.83	40.95	29.87	43.99
48	26.72	33.13	32.32	39.08	33.72	46.79	35.70	52.85	36.17	58.92
72	34.77	33.13	40.02	39.43	40.72	50.64	41.31	54.15	42.36	67.56

Conclusion

In the present article, nano-sized AgNPs are successfully synthesized by a simple, eco-friendly, cost-effective, and rapid green synthesis method by using the medicinal plant *B. lacera*, and characterized by different analytical techniques. The investigation embodied in this reports cytotoxic activity against adherent human lung carcinoma cell A549 using MTT assay, and the observed IC_{50} or MIC value was ~ 20 µg/mL. Hence, it may be used as an anticarcinogenic agent. Moreover, from a comparative study of antioxidant properties between medicinal plant *B. lacera leaf extract* and AgNPs, it is observed that AgNPs have superior antioxidant activity compared to the *B. lacer* plant, and the IC_{50} value of % radical scavenging activity for AgNPs was found to be ~ 6 µg/mL.

Acknowledgements The authors are highly grateful to the Head of Department (HoD), Department of Chemistry (DoC), University of Lucknow (UoL), Lucknow (UP), India, for providing basic infrastructure facilities, like UV–visible spectrophotometry and FT-IR spectroscopy for performing experimental work for my Ph.D. degree. The authors are also thankful to Vice-Chancellor Prof. Alok Kumar Rai of Lucknow University for partially assisting with funds through the Award of Chhatra Kalyan scholarship to PP funded by University of Lucknow, India. The authors are also grateful to the Advanced Materials Research Centre (AMRC), Kamand campus, IIT Mandi, H.P, the sophisticated analytical instrumentation facility (SAIF), All India Institute of Medical Science (AIIMS), New Delhi, and Birbal Sahni institute of Palaeosciences, Lucknow, UP, India, for providing X-ray diffraction, transmission electron microscopy and field emission scanning electron microscopy facilities, respectively. The authors are indebted to the Centre of Excellence scheme, Government of Uttar Pradesh, India, for cell culture facility in Molecular and Human Genetics Laboratory, Department of Zoology, University of Lucknow, Lucknow.

Author contribution All authors are equally contributed to data analysis, drafting or revising the article, gave final approval of the version to be published, and agree to be accountable for all aspects of the work.

Funding This research did not receive any specific grant from funding agencies in the public, commercial, or not-for-profit sectors.

Declarations

Conflict of interest The authors declared that there are no conflicts of interest.

References

Abdel-Aziz MS, Shaheen MS, EI-Nekeety AA, Abdel-Wahhab MA (2013) Antioxidant and antibacterial activity of silver nanoparticles using Chenopodium murale leaf extract. J Saudi Chem Soc 18:356–363. https://doi.org/10.1016/j.jscs.2013.09.011

Adewale OB, Egbeyemi KA, Onwuelu JO, Potts-Johnson SS, Anadozie SO, Fadaka AO, Osukoya OA, Aluko BT, Johnson J, Obafemi TO (2020) Biological synthesis of gold and silver nanoparticles using leaf extracts of Crassocephalum rubens and their comparative in vitro antioxidant activities. Heliyon 6:e05501. https://doi.org/10.1016/j.heliyon.2020.e05501

Ahmed FA, Rahman A, Mubassara S (2014) Phytochemical composition, antioxidant activity and cytotoxicity of Blumea lacera Linn. from two different habitats. Jahangirnagar Univ J Biol Sc 3:37–45. https://doi.org/10.3329/jujbs.v3i1.28276

Alahmad A, Feldhoff A, Bigall NC, Rusch P, Scheper T, Walter JG (2021) Hypericum perforatum L.-mediated green synthesis of silver nanoparticles exhibiting antioxidant and anticancer activities. Nanomaterials 11:487. https://doi.org/10.3390/nano11020487

AlNadhari S, Al-Enazi N, Alshehrei F, Ameen F (2020) A review on biogenic synthesis of metal nanoparticles using marine algae and its applications. Environ Res 194:110672. https://doi.org/10.1016/j.envres.2020.110672

Ameen F, Srinivasan P, Selvankumar T, Kamala-Kannan S, Al Nadhari S, Almansob A, Dawoud T, Govarthanan M (2019) Phytosynthesis of silver nanoparticles using Mangifera indica flower extract as bioreductant and their broad-spectrum antibacterial activity. Bioorgan Chem 88:102970. https://doi.org/10.1016/j.bioorg.2019.102970

Anandalakshmi K, Venugobal J, Ramasamy V (2016) Characterization of silver nanoparticles by green synthesis method using Pedalium murex leaf extract and their antibacterial activity. Appl Nanosci 6:399–408. https://doi.org/10.1007/s13204-015-0449-z

Aziz SB (2017) Investigation of metallic silver nanoparticles through UV–Vis and optical micrograph techniques. Int J Electrochem Sci. https://doi.org/10.20964/2017.01.22

Badán JA, Navarrete-Astorga E, Henriquez R, Martin F, Marotti RE, Ramos-Barrado JR, Dalchiele EA (2020) Optical properties of silver nanoparticles deposited onto silicon substrates by different soft-solution processing techniques. Opt Mater 100:1096651. https://doi.org/10.1016/j.optmat.2020.109651

BalaKumaran M, Ramachandran R, Balashanmugam P, Jagadeeswari S, Kalaichelvan PJMT (2022) Comparative analysis of antifungal, antioxidant and cytotoxic activities of mycosynthesized silver nanoparticles and gold nanoparticles. Mater Technol 37:411–421. https://doi.org/10.1080/10667857.2020.1854518

Braga LR, Rangel ET, Suarez PAZ, Machado F, Life S (2018) Simple synthesis of active films based on PVC incorporated with silver nanoparticles: evaluation of the thermal, structural and antimicrobial properties. Food Packag Shelf Life 15:122–129. https://doi.org/10.1016/j.fpsl.2017.12.005

Calderón-Jiménez B, Montoro Bustos AR, Pereira Reyes R, Paniagua SA, Vega-Baudrit JR (2022) Novel pathway for the sonochemical synthesis of silver nanoparticles with near-spherical shape and high stability in aqueous media. Sci Rep 12:1–17. https://doi.org/10.1038/s41598-022-04921-9

Gangwar C, Yaseen B, Kumar I, Singh NK, Naik RM (2021) Growth kinetic study of tannic acid mediated monodispersed silver nanoparticles synthesized by chemical reduction method and its characterization. ACS Omega 6:22344–22356. https://doi.org/10.1021/acsomega.1c03100

Gangwar C, Yaseen B, Nayak R, Praveen S, Singh NK, Sarkar J, Banerjee M, Naik RM (2022) Silver nanoparticles fabricated by tannic acid for their antimicrobial and anticancerous activity. Inorg Chem Commun 141:109532. https://doi.org/10.1016/j.inoche.2022.109532

Gangwar C, Yaseen B, Nayak R, Baker A, Bano N, Singh NK, Naik RM (2023) Madhuca longifolia leaves-mediated palladium nanoparticles synthesis via a sustainable approach to evaluate its biomedical application. Chem Pap. https://doi.org/10.1007/s11696-023-02688-5

Garibo D, Borbón-Nuñez HA, de León JND et al (2020) Green synthesis of silver nanoparticles using Lysiloma acapulcensis exhibit high-antimicrobial activity. Sci Rep 10:12805. https://doi.org/10.1038/s41598-020-69606-7

Guilger-Casagrande M, Germano-Costa T, Bilesky-José N, Pasquoto-Stigliani T, Carvalho L, Fraceto LF, de Lima R (2021) Influence of the capping of biogenic silver nanoparticles on their toxicity and mechanism of action towards Sclerotinia sclerotiorum. J Nanobiotechnol 19:1–18. https://doi.org/10.1186/s12951-021-00797-5

Htwe Y, Abdullah M, Mariatti M (2022) Water-based graphene/AgNPs hybrid conductive inks for flexible electronic applications. J Mater Res Technol 16:59–73. https://doi.org/10.1016/j.jmrt.2021.11.159

Hussein HA, Abdullah MA (2021) Novel drug delivery systems based on silver nanoparticles, hyaluronic acid, lipid nanoparticles and liposomes for cancer treatment. Appl Nanosci. https://doi.org/10.1007/s13204-021-02018-9

Jadhav K, Dhamecha D, Bhattacharya DD, Patil M (2016) Green and ecofriendly synthesis of silver nanoparticles: characterization, biocompatibility studies and gel formulation for treatment of infections in burns. J Photochem Photobiol B: Biol. https://doi.org/10.1016/j.jphotobiol.2016.01.002

Jadhav K, Deore S, Dhamecha DHRR, Jagwani S, Jalalpure S, Bohara R (2018) Phytosynthesis of silver nanoparticles: characterization, biocompatibility studies, and anticancer activity. ACS Biomater Sci Eng. https://doi.org/10.1021/acsbiomaterials.7b00707

Jagwani S, Jalalpure S, Dhamecha D, Jadhav K, Bohara R (2020) Pharmacokinetic and pharmacodynamic evaluation of resveratrol loaded cationic liposomes for targeting hepatocellular carcinoma. ACS Biomater Sci Eng. https://doi.org/10.1021/acsbiomaterials.0c00429

Jha M, Shimpi NG (2018) Green synthesis of zero valent colloidal nanosilver targeting A549 lung cancer cell: in vitro cytotoxicity. J Genetic Eng Biotechnol 16:115–124. https://doi.org/10.1016/j.jgeb.2017.12.001

Karthik P, Singh SP (2015) Conductive silver inks and their applications in printed and flexible electronics. RSC Adv 5:77760–77790. https://doi.org/10.1039/C5RA12013F

Khalir WKAWM, Shameli K, Jazayeri SD, Othman NA, Jusoh NWC, Hassan NM (2020) Biosynthesized silver nanoparticles by aqueous stem extract of Entada spiralis and screening of their biomedical activity. Front Chem 8:620. https://doi.org/10.3389/fchem.2020.00620

Khatoon UT, Rao GN, Mohan KM, Ramanaviciene A, Ramanavicius A (2017) Antibacterial and antifungal activity of silver nanospheres synthesized by tri-sodium citrate assisted chemical approach. Vacuum 146:259–265. https://doi.org/10.1016/j.vacuum.2017.10.003

Kumar I, Gangwar C, Yaseen B, Pandey PK, Mishra SK, Naik RM (2022a) Kinetic and mechanistic studies of the formation of silver nanoparticles by nicotinamide as a reducing agent. ACS Omega 7:13778–13788. https://doi.org/10.1021/acsomega.2c00046

Kumar I, Nayak R, Chaudhary LB, Pandey VN, Mishra SK, Singh NK, Srivastava A, Prasad AS, Naik RM (2022b) Fabrication of α-Fe_2O_3 nanostructures: synthesis, characterization, and their promising application in the treatment of carcinoma A549 lung cancer cells. ACS Omega 25:21882–21890. https://doi.org/10.1021/acsomega.2c02083

Labulo AH, David OA, Terna AD (2022) Green synthesis and characterization of silver nanoparticles using Morinda lucida leaf extract and evaluation of its antioxidant and antimicrobial activity. Chem Pap. https://doi.org/10.1007/s11696-022-02392-w

Lugani Y, Sooch BS, Singh P, Kumar S (2021) Nanobiotechnology applications in food sector and future innovations. Microbial biotechnology in food and health. Elsevier, pp 197–225. https://doi.org/10.1016/B978-0-12-819813-1.00008-6

Mamdouh S, Mahmoud A, Samir A, Mobarak M, Mohamed T (2022) Using femtosecond laser pulses to investigate the nonlinear optical properties of silver nanoparticles colloids in distilled water synthesized by laser ablation. Physica B: Condensed Matter 631:413727. https://doi.org/10.1016/j.physb.2022.413727

Mendhulkar VD, Patade P, Vakil M (2016) Elicitation of flavonoids in Blumea lacera (Burm.f.) DC. Cell culture using chemical elicitor, salicylic acid and biological elicitor, aspergillus Niger. Int J Curr Res Biosci Plant Biol 3(11):85–91. https://doi.org/10.20546/ijcrbp.2016.311.013

Mishra SK, Tripathi U, Awasthi RR, Shukla R, Kumar I, Naik RM, Mishra D (2021) CTAB mediated synthesis of ZnO nanoparticles: Structural, optical and enhanced blue-green optical emission. Mater Today: Proc 46:2229–2234. https://doi.org/10.1016/j.matpr.2021.03.481

Mistry H, Thakor R, Patil C, Trivedi J, Bariya H (2020) Biogenically proficient synthesis and characterization of silver nanoparticles employing marine procured fungi Aspergillus brunneoviolaceus along with their antibacterial and antioxidative potency. Biotechnol Lett 43:307–316. https://doi.org/10.1007/s10529-020-03008-7

Mosmann T (1983) Rapid colorimetric assay for cellular growth and survival: application to proliferation and cytotoxicity assays. J Immunol Methods 65:55–63. https://doi.org/10.1016/0022-1759(83)90303-4

Paaniappan P, Satishkumar G, Sankar R (2015) Fabrication of nanosilver particles using Cymodocea serrulata and its cytotoxicity effect against human lung cancer A549 cells line. Spectro Acta Part A Mol Biomol Spectrosc 138:885–890. https://doi.org/10.1016/j.saa.2014.10.072

Padmini R, Nallal UM, Razia M, Sivaramakrishnan S, Alodaini HA, Hatamleh AA, AL-Dosary MA, Rangnathan V, Chung WJ (2022) Cytotoxic effect of silver nanoparticles synthesized from ethanolic extract of Allium sativum on A549 lung cancer cell line. J King Saud Univ Sci. https://doi.org/10.1016/j.jksus.2022.102001

Pulit-Prociak J, Grabowska A, Chwastowski J, Majka TM, Banach M (2019) Safety of the application of nanosilver and nanogold in topical cosmetic preparations. Coll Surf B: Biointerfaces 183:110416. https://doi.org/10.1016/j.colsurfb.2019.110416

Ratan ZA, Haidere MF, Nurunnabi M, Shahriar SM, Ahammad AJS, Shim YY, Reaney MJT, Cho JY (2020) Green chemistry synthesis of silver nanoparticles and their potential anticancer effects. Cancers (basel) 12:885. https://doi.org/10.3390/cancers12040855

Ravichandrana V, Vasanthi S, Shalini S, Shah SAA, Haris R (2016) Green synthesis of silver nanoparticles using Atrocarpus altilis leaf extract and the study oftheir antimicrobial and antioxidant activity. Mater Lett 180:264–267. https://doi.org/10.1016/j.matlet.2016.05.172

Sankar R, Karthik A, Prabu A, Karthik S, Shivashangari K S, Ravikumar V (2013) Origanum vulgare mediated biosynthesis of silver nanoparticles for its antibacterial and anticancer activity. Coll Surf B: Biointerfaces 108:80–84. https://doi.org/10.1016/j.colsurfb.2013.02.033

Selvan DA, Mahendiran D, Kumar RS, Rahiman AK (2018) Garlic, green tea and turmeric extracts-mediated green synthesis of silver nanoparticles: phytochemical, antioxidant and in vitro cytotoxicity studies. J Photochem Photobiol, B 180:243–252. https://doi.org/10.1016/j.jphotobiol.2018.02.014

Shahcheraghi N, Golchin H, Sadri Z, Tabari Y, Borhanifar F, Makani S (2022) Nano-biotechnology, an applicable approach for sustainable future. Biotech 12:65. https://doi.org/10.1007/s13205-021-031089

Shalini A, Priya K, Kothai S, Kannaiyan P, Anbalagan G, Jaisankar V (2022) Synthesis and characterisation of graphene oxide decorated gold nano particles and their application towards antibacterial activity. Chem Pap. https://doi.org/10.1007/s11696-022-02375-x

Sharma D, Kanchi S, Bisetty K (2015) Biogenic synthesis of nanoparticles: a review. Arab J Chem 12:3576–3600. https://doi.org/10.1016/j.arabjc.2015.11.002

Shen L, Chen M, Hu L, Chen X, Wang J (2013) Growth and stabilization of silver nanoparticles on carbon dots and sensing application. Langmuir 29:16135–16140. https://doi.org/10.1021/la404270w

Singh I, Al-Wahaibi LH, Srivastava R, Prasad O, Pathak SK, Kumar S, Parveen S, Banerjee M, El-Emam AA, Sinha L (2020) DFT study on the electronic properties, spectroscopic profile, and biological activity of 2-Amino-5-trifluoromethyl-1,3,4-thiadiazole with anticancer properties. ACS Omega 5(46):30073–30087. https://doi.org/10.1021/acsomega.0c04474

Sreelekha E, George B, Shyam A, Sajina N, Mathew B (2021) A comparative study on the synthesis, characterization, and antioxidant activity of green and chemically synthesized silver nanoparticles. BioNanoScience 11:489–496. https://doi.org/10.1007/s12668-021-00824-7

Sytu MRC, Camacho DH (2018) Green synthesis of silver nanoparticles (AgNPs) from Lenzites betulina and the potential synergistic effect of AgNPs and capping biomolecules in enhancing antioxidant activity. BioNanoScience 8:835–844. https://doi.org/10.1007/s12668-018-0548-x

Thampi N, Shalini VJ (2015) Bio-prospecting the in-vitro antioxidant and anti-cancer activities of silver nanoparticles synthesized from the leaves of syzygium samarangense. Int J Pharm Pharm Sci 7:269–274

Venkatesan B, Subramanian V, Tumala A, Vellaichamy E (2014) Rapid synthesis of biocompatible silver nanoparticles using aqueous extract of Rosa damascena petals and evaluation of their anticancer activity. Asian Pac J Trop Med 7S1:S294-300. https://doi.org/10.1016/s1995-7645(14)60249-2

Wu J, Zhao N, Zhang X, Xu J (2012) Cellulose/silver nanoparticles composite microspheres: eco-friendly synthesis and catalytic application. Cellulose 19:1239–1249. https://doi.org/10.1007/s10570-012-9731-3

Xu S, Zhu Q, Lin X, Lin W, Qin Y, Li Y (2020) The phase behavior of n-ethylpyridinium tetrafluoroborate and sodium-based salts ATPS and its application in 2-chlorophenol extraction Chinese. J Chem Eng. https://doi.org/10.1016/j.cjche.2020.07.024

Yadav P, Pandey SK, Shama P, Kumar S, Banerjee M, Sethi A (2021) Experimental and theoretical investigation of synthesized pregnenolone derivatives via palladium catalyzed cross coupling reactions, their anticancer activity against lung cancer cells. J Mol Struct 1245:131115. https://doi.org/10.1016/j.molstruc.2021.131115

Yaseen B, Gangwar C, Kumar I, Sarkar J, Naik RM (2022) Detailed kinetic and mechanistic study for the preparation of silver nanoparticles by a chemical reduction method in the presence of a neuroleptic agent (Gabapentin) at an Alkaline pH and its characterization. ACS Omega 7:5739–5750. https://doi.org/10.1021/acsomega.1c05499

Zhu Q, Xu S, Wu W, Qi Y, Lin Z, Li Y, Qin Y (2022) Hierarchical hollow zinc oxide nanocomposites derived from morphology-tunable coordination polymers for enhanced solar hydrogen production. Angewandte Chemie Int Edition. https://doi.org/10.1002/anie.202205312

Publisher's Note Springer Nature remains neutral with regard to jurisdictional claims in published maps and institutional affiliations.

Springer Nature or its licensor (e.g. a society or other partner) holds exclusive rights to this article under a publishing agreement with the author(s) or other rightsholder(s); author self-archiving of the accepted manuscript version of this article is solely governed by the terms of such publishing agreement and applicable law.